A MATHEMATICAL MODEL DEVELOPMENT OF A FLAT PLATE SOLAR COLLECTOR OPERATING IN TRANSIENT REGIME

Ricieri Fornazari Filho, ricieri.fornazari@gmail.com
Santiago del Rio Oliveira, santiago@feb.unesp.br
São Paulo State University, Bauru Campus, Engenheiro Luiz Edmundo Carrijo Coube Avenue 14-01, Vargem Limpa District, ZIP CODE 17033-360.

Abstract. *Solar energy is becoming an alternative in front of the scarcity of fossil fuel reserves. One of the simplest and most direct applications of this energy is the conversion of solar radiation into heat, which can be used in water heating systems. A solar heating system widely used is the solar flat plate collector. A lot of research has been done in order to analyze the operation of a solar flat plate collector and increase their thermal efficiency. The objective of this research project is to develop a one-dimensional mathematical model to simulate transient processes occurring in flat plate collectors operating with liquid. The model considers thermophysical properties and heat transfer coefficients time dependent, and is based on the solution of differential equations involving the conservation of energy to the glass cover, the air space between the glass cover and the absorber, absorber, working fluid and insulation. The differential equations are solved using an implicit finite difference method in an iterative scheme using MATLAB. The proposed solution solves numerically the model developed considering transient conditions in the solar collector, calculating the transient temperature distribution for any cross section of the collector at a given time. As expected the highest temperatures have been reached in the absorber along the processing time, its high thermal conductivity results in rapid thermal response from the recirculating fluid. It has also been noted that the insulation temperature variation is very small, due to the low thermal conductivity of the material, in order to diminish the heat losses. Time dependent volumetric flow, variable ambient temperature, variable solar radiation have been considered. The model does not require the temperature history as input, being, therefore, suitable for low and high operation flow.*

Keywords*: solar collector, finite differences, solar energy*.

1. INTRODUCTION

Flat plate solar collectors are the most common type of solar collectors for residential water heating and ambient heating systems. A common flat plate collector, Fig. 1, consists of an absorber plate contained in an insulated box with transparent cover sheets (glasses). The absorber is, generally, a high thermal conductivity metallic flat plate, such as copper or aluminum, with integrated or connected tubes. Its surface is coated with a selective material to maximize energy absorption from radiation, while minimizing the emission of this type of energy.

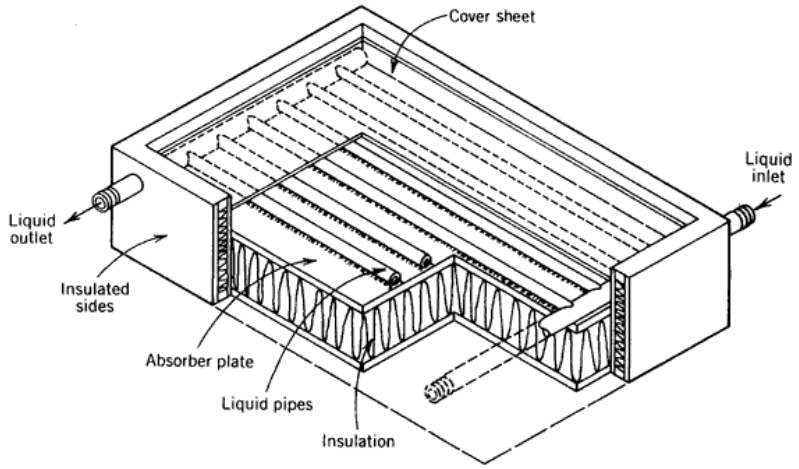

Figure 1. Transversal section of a flat plate solar collector for liquids. Source: http://www.powerfromthesun.net.

Considering the exhaustible fossil fuels and the degradation caused by these, Kalogirou (2004) presented that the use of solar energy avoids great amount of green house gases. For a residential water heating system the savings are about 80% when compared solar heating to conventional electrical or Diesel systems. In internal space heating savings are about 40%. The work studied different systems and concluded those to be financially promising, and, most important, significant environment preservation by avoiding green house gases.

Studies conducted by Delgado and Campbell (2014) showed that observation and recording of relevant variables , such as temperature , wind speed and solar radiation over a year, as well as the history of the working fluid temperature

inside the collector and storage tank every five minutes interval allowed the prediction of system performance for a higher capacity throughout the year. In terms of economic analysis, there was a saving of 80% in residential energy, with return on investment in about five years.

A glassed flat plate collector with selective black chrome coated absorber and a low wall conductance horizontal storage were combined in order to set up a high performance thermosyphon system in the study conducted by (Zelzouli et al., 2014). During the test period, effect of different inlet water temperatures on the collector performance have been studied and results have shown that the collector can reach a high efficiency and high outlet water temperature even for elevated inlet water temperatures. Subsequently, long term system performance is estimated by using a developed numerical model. The proposed model, accurate and gave a good agreement with experimental results, allowed to describe the heat transfer in the storage. It has also shown that the long-term performances are strongly influenced by losses from the storage than losses from the collector.

The main objectives of this project are:

- To develop a dynamic mathematical model for a flat plate solar collector with one glass cover in parallel with the channel arrangements under transient conditions;
- To develop a numeric solution for the mathematical model, using MATLAB for the code, in order to obtain the transient temperature distribution for any section of the solar collector in a determined instant of time;
- To obtain numeric solutions for a group of parameters previously determined.

2. MATHEMATICAL MODELING AND NUMERIC MODEL

2.1. Physical problem description

In the proposed model, the control volume analyzed for a flat plate solar collector contains a control surface divided into five nods (glass cover, air space, absorber, fluid and insulation) perpendicular to fluid flow direction.

The ruling equations for this model can be deducted from the First Law of Thermodynamics application for each zone of the control volume mentioned above. For one-dimensional and transient heat transfer, the global energy balance can be written as in Eq. (1):

$$\frac{dE_{accu}}{dt} = \dot{E}_{in} - \dot{E}_{out} + \dot{E}_{g} \tag{1}$$

where $\frac{dE_{accu}}{dt}$ is the accumulated energy variation rate in the control volume, $\dot{E}_{in}$ is the energy ratio that enters the control volume, $\dot{E}_{out}$ is the energy ratio that exits the control volume and $\dot{E}_{g}$ is the volumetric generated energy ratio inside the control volume.

An uniform mass flow of the working fluid, $\dot{m}_f$, can be defined as a function of the total mass flow in the solar collector entrance, $\dot{m}_t$, and the number of tubes in the collector, *n*:

$$\dot{m}_f = \frac{\dot{m}_t}{m} \tag{2}$$

To simplify the solar collector analysis, the following assumptions have been made:

- Uniform mass flow inside the tubes;
- One-dimensional heat transfer through the layers;
- There is no heat transfer in the flow direction, in other words, energy by mass transference in this direction;
- Glass and Insulation properties have constant value;
- The losses from the collector top and bottom are the same for the same ambient temperature;
- Volumetric energy generation inside the collector is zero.

2.2. Finite differences approximation

The differential equations to be presented have been numerically solved through the implicit finite differences technique. The implicit expression of finite differences equations can be deducted by Eq. (3) to approximate the derivatives in time:

$$\frac{dT_m}{dt} \approx \frac{T_{m,j}^{t+\Delta t} - T_{m,j}^{t}}{\Delta t} \tag{3}$$

where *m* is replaced by *g* (glass cover), *a* (air), *abs* (absorber), *i* (insulation) and *f* (working fluid). The index *j* stands for the number of the node on the flow direction (*z*). According to Eq. (3), all the temperatures are determined in the instant of time $t + \Delta t.$.

2.3. Finite differences equations

The energy balance to an open system involving the glass cover is illustrated in Fig. 2 and Eq. (4):

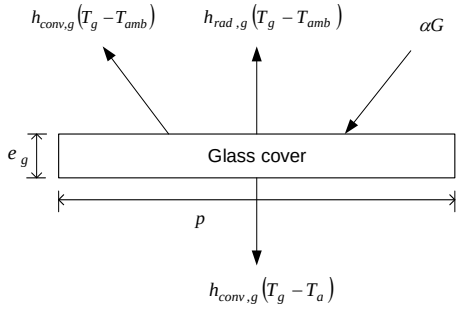

Figure 2. Energy balance for the glass cover.

$$\rho_g V_g c_g \frac{dT_g}{dt} = \left[h_{comb,g-amb}\left(T_{amb} - T_g\right) + h_{rad,g-abs}\left(T_{abs} - T_g\right) + h_{conv,g-a}\left(T_a - T_g\right) + \alpha G\right]\left(p\Delta z\right) \tag{4}$$

In Eq. (4) ρ_g is the glass density, V_g is the glass volume, c_g is the glass specific heat, α is the glass absorptivity, G is the solar radiation flux, $h_{comb,g-amb}$ is the combined radiation and convection heat transfer coefficient, h_{conv} is the convection coefficient, h_{rad} is the radiation coefficient, T_g is the glass temperature, T_{amb} is the ambient temperature, T_{abs} is the absorber temperature, T_a is the air temperature and $\left(p\Delta z\right)$ is the orthogonal area to the heat flux.

Equation (4) can be discretized using Eq. (3) combined with the nodal index for the combined, radiation and convection heat coefficients and for solar irradiation:

$$\rho_g V_g c_g \frac{T_{g,j}^{t+\Delta t} - T_{g,j}^{t}}{\Delta t} = [h_{comb,g-amb,j}\left(T_{amb}^{t+\Delta t} - T_{g,j}^{t+\Delta t}\right) + h_{rad,g-abs,j}\left(T_{abs,j}^{t+\Delta t} - T_{g,j}^{t+\Delta t}\right) + h_{conv,g-a,j}\left(T_{a,j}^{t+\Delta t} - T_{g,j}^{t+\Delta t}\right) + \alpha G^{t+\Delta t}](p\Delta z) \tag{5}$$

Collecting the terms with $T_{g,j}^{t+\Delta t}$ and setting the following variables:

$$B_j = \frac{h_{comb,g-amb,j}}{\rho_g e_g c_g} \qquad C_j = \frac{h_{rad,g-abs,j}}{\rho_g e_g c_g} \qquad D_j = \frac{h_{conv,g-a,j}}{\rho_g e_g c_g} \qquad E = \frac{\alpha}{\rho_g e_g c_g} \qquad F_j = 1/\Delta t + B_j + C_j + D_j$$

The final equation for the glass temperature is written as:

$$T_{g,j}^{t+\Delta t} = \frac{1}{F_f \Delta t} T_{g,j}^{t} + \frac{B_j}{F_f} T_{amb}^{t+\Delta t} + \frac{C_j}{F_f} T_{abs,j}^{t+\Delta t} + \frac{D_j}{F_f} T_{a,j}^{t+\Delta t} + \frac{E}{F_f} G^{t+\Delta t},\ j = 1,2,...N \tag{6}$$

The same procedure above has been used to write the finite difference temperature for the other collector structures. The final equation for the air space, absorber plate, insulation and working fluid are presented, in that order:

$$T_{a,j}^{t+\Delta t} = \frac{1}{I_j \Delta t} T_{a,j}^{t} + \frac{G_j}{I_j} T_{g,j}^{t+\Delta t} + \frac{H_j}{I_j} T_{abs,j}^{t+\Delta t} \tag{7}$$

$$G_j = \frac{h_{conv,a-g,j}}{\rho_a(T_a)_j e_a c_a(T_a)_j} \qquad H_j = \frac{h_{conv,a-abs,j}}{\rho_a(T_a)_j e_a c_a(T_a)_j} \qquad I_j = 1/\Delta t + G_j + H_j$$

$$T_{abs,j}^{t+\Delta t} = \frac{1}{Q_j \Delta t} T_{abs,j}^{t} + \frac{K_j}{Q_j} G^{t+\Delta t} + \frac{L_j}{Q_j} T_{g,j}^{t+\Delta t} + \frac{M_j}{Q_j} T_{a,j}^{t+\Delta t} + \frac{O_j}{Q_j} T_{f,j}^{t+\Delta t} + \frac{P_j}{Q_j} T_{i,j}^{t+\Delta t},\ j = 1,2,...N \tag{8}$$

$$J_j = \rho_{abs}(T_{abs})_j[\,pe_{abs} + \pi(r_{ext}^2 - r_{\text{int}}^2)]c_{abs}(T_{abs})_j \qquad K_j = \frac{(\tau\alpha)p}{J_j} \qquad L_j = \frac{h_{rad,abs-g,j}\,p}{J_j} \qquad M_j = \frac{h_{conv,abs-a,j}\,p}{J_j}$$

$$O_j = \frac{h_{conv,f,j}\pi d_k}{J_j} \qquad P_j = \frac{k_i p}{e_i J_j} \qquad Q_j = 1/\Delta t + L_j + M_j + O_j + P_j$$

$$T_{i,j}^{t+\Delta t} = \frac{1}{X_j \Delta t}T_{i,j}^{t} + \frac{V_j}{X_j}T_{abs,j}^{t+\Delta t} + \frac{W_j}{X_j}T_{amb,j}^{t+\Delta t},\ j = 1,2,...N \tag{9}$$

$$V_j = \frac{k_i}{\rho_i e_i^2 c_i} \qquad W_j = \frac{h_{comb,i-amb,j}}{\rho_i e_i c_i} \qquad X_j = 1/\Delta t + V_j + W_j$$

$$T_{f,j}^{t+\Delta t} = \frac{1}{U_j \Delta t}T_{f,j}^{t} + \frac{R_j}{U_j}T_{abs,j}^{t+\Delta t} + \frac{S_j}{U_j \Delta z}T_{f,j-1}^{t+\Delta t} \tag{10}$$

$$R_j = \frac{h_{f,conv,j}\pi d_k}{\rho_f(T_f)_j Ac_f(T_f)_j} \qquad S_j = \frac{\dot{m}_f}{\rho_f(T_f)_j A} \qquad U_j = 1/\Delta t + R_j + S_j/\Delta z$$

3. NUMERICAL MODEL

The model to solve the mathematical modeling has been developed considering a solar collector with a single glass cover. All physical dimensions are input data, what makes the model suitable for any single covered flat plate solar collector. The fluid conditions on inlet, initial temperature, climate data, time of process, initial pitch and time interval for calculation are also required as input information. An initial convergence criteria is set to adjust mass flow, time and space pitch, following to the calculation of the properties, then heat transfer coefficients, then the global coefficients (*A, B...X*) for each structure in each instant of time and node. Finally, the temperatures of the glass cover, air space, working fluid, absorber and insulation are calculated at a specified node. If all the nodes converged and the instant of time is the total time set, the results are stored and displayed.

The code has been written in MATLAB. It solves the model and calculates the transient temperatures distribution for any transversal section beginning at time $t = 0$. The process is carried out for a total time provided by the user.

4. RESULTS AND DISCUSSION

The first part of results is the analysis of the numerical code convergence, followed by numerical results obtained for the temperatures history. The input data for the model are shown in the following table:

Table 1. Input data for the numerical model

$d_i = 9.5$ (mm)	$c_v = 720$ (J/kg.K)	$\rho_{abs} = 8795$ (kg/m³)
$L = 1900$ (mm)	$c_{iso} = 1030$ (J/kg.K)	$c_a = 1.005 \times 10^3$ (J/kg.K)
$p = 0.127$ (m)	$\rho_v = 2500$ (kg/m³)	$\sigma = 5.67 \times 10^{-8}$ (W/m².K⁴)
$d_e = 10.0$ (mm)	$\rho_{iso} = 70$ (kg/m³)	$\varepsilon_v = 0.88$
$e_v = 3.81$ (mm)	$\alpha = 0.005$	$\varepsilon_{iso} = 0.05$
$e_{iso} = 50.8$ (mm)	$\tau\alpha = 0.861$	$g = 9.81$ (m/s²)
$e_{abs} = 0.015$ (m)	$k_{iso} = 0.035$ (W/m.K)	$\theta = 45^{o}$
$e_{ar} = 0.025$ (mm)	$c_{abs} = 385$ (J/kg.K)	$a = 1.9$ (m)
$b = 0.92$ (m)	$L = a$	$U_\infty = 1.5$ (m/s)
$\nu_\infty = 1.5743 \times 10^{-5}$ (m²/s)	$k_\infty = 0.0262$ (W/m.K)	$\text{Pr}_\infty = 0.071432$

The temperatures distribution obtained through the MATLAB developed code have been tested for different number of nodes (n = 4, 6, 8, 12, 24, 48 and 72) along the flow direction. Figure 3 exhibits the outlet collector temperature numerically obtained for different number of nodes for a constant volumetric flow of 0.34 m³/h, (1.5 GPM).

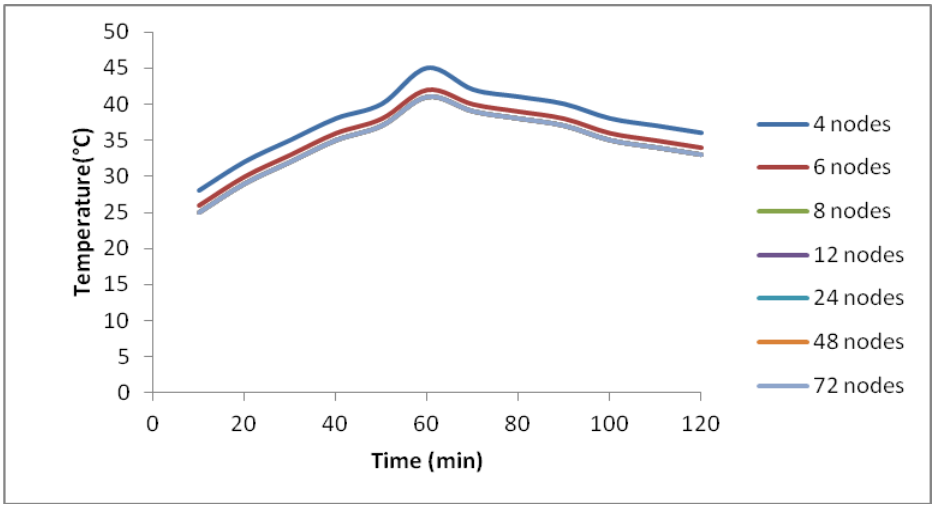

Figure 3. Outlet temperature history for different number of nodes with volumetric flow of 0.34 m³/h.

As it can be concluded from Fig. 3, the proposed method converges when the number of nodes equals 12. It should be noted that the curves from 8 to 72 nodes are overlapping and, thus, 12 nodes have been considered as the convergence criterion. Table 2 exhibits the processing time and the error range in temperatures obtained through the 72 nodes model. However, results obtained suggest to limit the number of nodes as 24, in order to optimize the processing time with acceptable error compared to the optimal case of 72 nodes model.

Table 2. Error range in comparison to 72 nodes and processing time for different number of nodes for a volumetric flow of 0.34 m³/h.

	Number of nodes (n)						
	4	6	8	12	24	48	72
Time pitch (s)	3.8	2.3	1.6	1.0	0.5	0.24	0.16
Error range (°C)	± 0.64	± 0.06	± 0.06	± 0.05	± 0.02	± 0.01	± 0
Processing time (s)	26.35	33.30	53.18	80.25	194.5	502.4	924

In order to analyze the code response to transient inlets, once this type of input could complicate the model convergence, solar irradiation have been described by two different pitch functions. The first inlet simulates a sudden change of solar irradiation after one hour while the second simulates a sudden change earlier, after 30 minutes. Figure 4 shows the working fluid outlet temperature values calculated for both cases, which have been simulated for 24 nodes under the same conditions, except for the pitch function of solar irradiation.

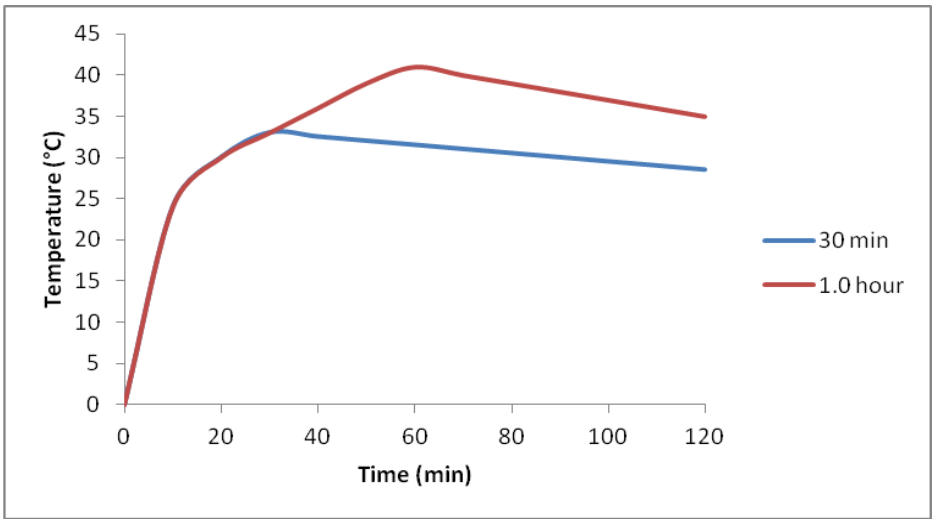

Figure 4. Outlet temperatures for different inlet of solar irradiation.

Figure 5 shows the working fluid outlet temperature history for three different time pitch: 0.1 second, 0.5 second (maximum pitch satisfying the stability condition for 0.34 m³/h and 24 nodes), and 2.0 seconds.

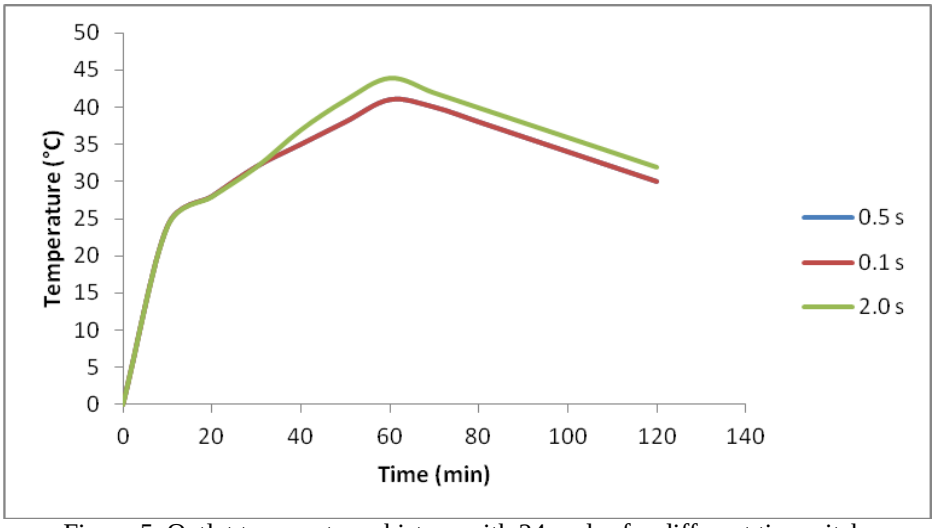

Figure 5. Outlet temperatures history with 24 nodes for different time pitch.

The smallest pitch of 0.1 second results in the greatest stability among other time pitch as shown in Fig. 5, although highest computational time. Time pitch of 2.0 seconds has caused the worst stability case although shortest computational time. The best solution was to use the longest time that still satisfies the stability condition (0.5 second, in this case), since it gives close results to the 0.1 second case with acceptable processing time.

Table 3 exhibits the error range and time processing for each case compared to the 0.1 second case.

Table 3. Error range and processing time for the same number of nodes with different time pitch compared to the 0.1 second case

	Time pitch Δt (s)		
	0.1	0.5	2.0
Error range (°C)	0	± 0.01	± 2.53
Processing time (s)	2354	195.4	47

The outlet temperature history for the solar collector components, such as glass cover, air space, absorber, working fluid and insulation at the transversal section represented by node 12 (L = 0.95 m) are presented in Fig. 6. The results have been obtained for a volumetric flow of 0.34 m³/h, 24 nodes and time pitch of 0.5 second for stability.

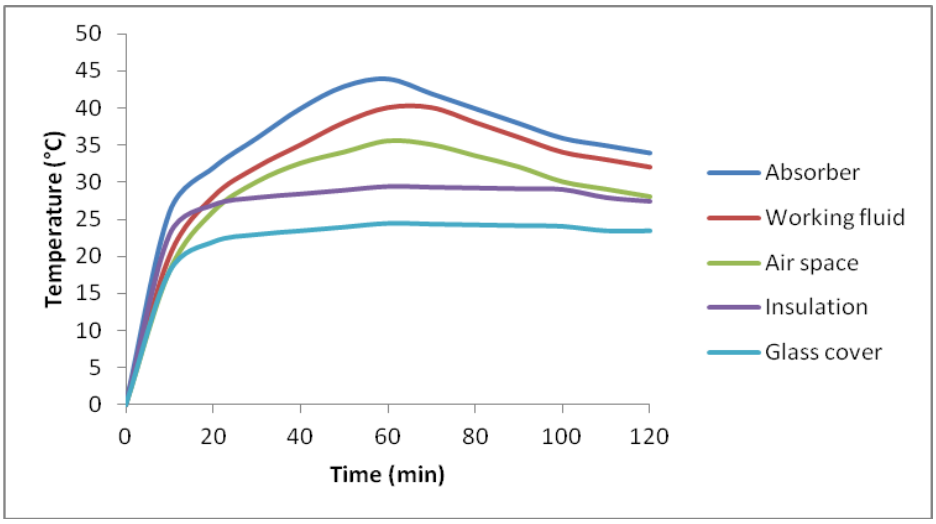

Figure 6. Temperature history for the transversal section analyzed, at node 12.

As it were expected, the highest temperatures have been reached in the absorber plate along the processing time, once the primal objective of the absorber plate is to absorb as much as possible of the solar radiation through the glass, lose little energy as possible from its top to the atmosphere and from its bottom by the insulation and transfer the heat retained to the working fluid. The absorber high thermal conductivity results in a rapid thermal response of the working fluid as a result of some temperature variation on the absorber.

It can also be seen that the temperature varies very little on the insulation , which is due to the low thermal conductivity of the insulating material, once it is a necessity to reduce heat losses from the system. The purpose of the glass cover is to admit the maximum solar radiation as possible and to reduce the heat loss from the top of the collector . The glass cover material used has a high transmittance and a low absorption coefficient. Based on the temperature history obtained for the cover , this component has the lowest temperature variation over time , being, therefore, efficient for its purpose.

The temperature variation in the air space is due to the heat transferred by convection and radiation from the absorber. That loss could certainly be reduced if it were possible to create vacuum inside the collector instead of the air space. Figure 7 shows the temperatures history obtained by the 24 nodes numerical solution for a volumetric flow of 0.34 m³/h on the inlet, outlet and half the length in the flow direction (node 12):

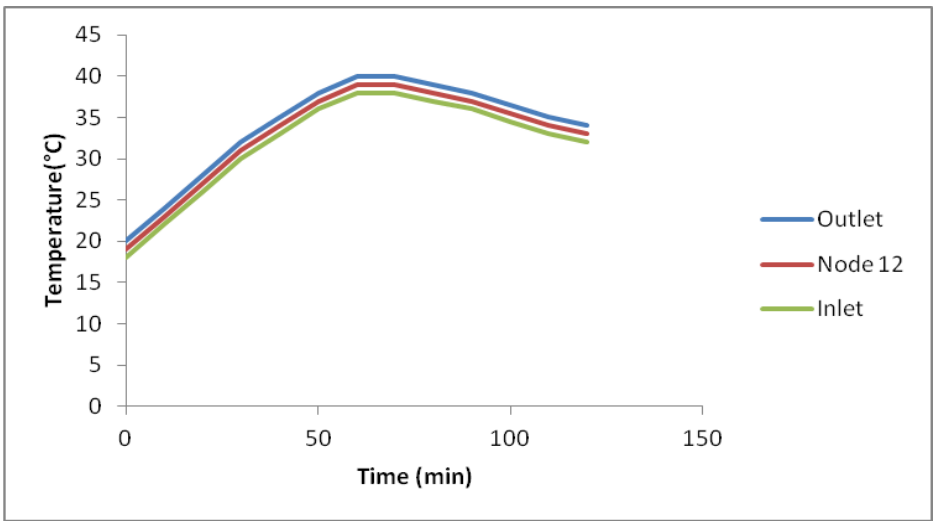

Figure 7. Temperatures history of the working fluid at inlet, half length and outlet of the collector.

On Table 4 it can be seen the data for solar radiation and temperature used in computer simulation. These data have been obtained directly from the Meteorology Center of Bauru, IPMET, for different days, and an average of the collected data have been calculated:

Table 4. Solar irradiation and ambient temperature for simulation

Time (min)	Irradiation (W/m^2)	Ambient temperature (^{o}C)
0	0	24
15	849.6	35
30	854.3	35
45	897.1	38
60	892.6	37
75	175.6	35
90	0	31
105	0	29
120	0	28

5. CONCLUSIONS

A transient one-dimensional mathematical model with time dependent properties has been developed to simulate the

process of solar energy collecting. The thermophysical properties of the air space , the absorber plate and the working fluid were calculated as time-dependent as well as heat transfer coefficients.

To solve the differential equations obtained an implicit finite difference scheme has been used and the model was able to simulate transient processes that occur in a flat plate solar collector. Time dependent volumetric flow was taken into consideration as well as variable temperature and variable solar radiation.

The proposed solution method has been implemented using MATLAB. The code mathematically solves the model and allows to calculate the temperatures history for each transversal section of the collector at any point along the flow direction of the working fluid. The numerical model has been able to solve the proposed situation even with a non-uniform distribution of solar radiation. It does not require the temperatures history as an input, being, therefore, suitable for low and high operating flow.

6. REFERENCES

Delgado, R. and Campbell, H.E., 2014. "Adaptation and sizing of solar water heaters in desert areas: for residential and hotels". Energy Procedia, Vol. 57, pp. 2725-2732.

Kalogirou, S.A., 2004. "Environmental benefits of domestic solar energy systems". Energy Conversion and Management, Vol. 45, pp. 3075-3092.

Zelzouli, K., Guizani, A. and Kerkeni, C., 2014. "Numerical and experimental investigation of thermosyphon water heater". Energy Conversion and Management, Vol. 79, pp. 913-922.

7. RESPONSIBILITY NOTICE

The authors are the only responsible for the printed material included in this paper.